Applied Magnetic Resonance (2022) 53:979–988
https://doi.org/10.1007/s00723-021-01419-x

Applied
Magnetic Resonance

ORIGINAL PAPER

EPR Study of New Bis-methano[60]fullerenes in Liquid

R. B. Zaripov[1] · I. T. Khairutdinov[1] · G. M. Fazleeva[2] · L. N. Islamova[2] · V. P. Gubskaya[2] · I. A. Nuretdinov[2]

Received: 26 April 2021 / Revised: 10 August 2021 / Accepted: 13 August 2021 /
Published online: 22 August 2021

Abstract

Methano[60]fullerenes with two and four nitroxide radicals are studied by EPR spectroscopy. It is shown that nitroxide derivatives of fullerene C_{60} undergo conformational changes in liquid solution. It is established that transitions between the two conformations take place in the case of the biradical adduct of C_{60} fullerene. For the tetraradical adduct in the trans-3 position, it is shown that the biradicals do not interact and behave independently; therefore, the two-conformational model provides a good description of the experimental data. A more complicated situation is implemented for the tetraradical adduct in the equatorial position. The biradicals are not independent for this system, and their interaction leads to an increase in the number of possible conformations. Thermodynamic parameters for these systems are calculated.

1 Introduction

Since being discovered, fullerenes attracted much attention of researchers worldwide. Interest is mainly due to the fact that this amazing molecule and its derivatives are used in many fields, e.g., fullerene is applied as an additive to reduce friction of the contacting parts, as a solar cell, as additives intumescent flame retardant paints, carbon nanotubes, superconductors, etc. It should be noted that recently the usage of fullerenes or rather their derivatives found new applications in pharmacology [1–6]. Since fullerene C_{60} is hydrophobic, chemists are faced with the task of obtaining water-soluble fullerene derivatives [7–9]. This task can be achieved by varying the attached chemical groups. As a result, new effective fullerene derivatives may

✉ I. A. Nuretdinov
zaripov.ruslan@gmail.com

[1] Zavoisky Physical-Technical Institute, FRC Kazan Scientific Center of RAS, Kazan, Russian Federation

[2] Arbuzov Institute of Organic and Physical Chemistry, FRC Kazan Scientific Center of RAS, Kazan, Russian Federation

appear for the treatment of human diseases, e.g., human immunodeficiency virus [10–12].

Fullerene C_{60} is a convenient template for attaching a large number of stable free radicals in different relative positions on the fullerene shell and for studying their interaction [13–16]. A new class of nitroxide fullerene derivatives is promising for obtaining previously unknown anticancer drugs and for studying the pharmacokinetics of fullerene derivatives in a living organism using electron paramagnetic resonance (EPR) spectroscopy. In [13], fullerene was successfully used to prepare, according to our proposed method [14], bis- and hexa-nitroxide derivatives of fullerene C_{60}, which the authors used as active catalysts for the oxidation of primary and secondary alcohols to aldehydes and ketones. Moreover, it was shown recently that fullerene derivatives with pharmacophoric groups can be used as a supplement to medicine to treat leukemia. For example, I.A. Nuretdinov et al. [14] (Arbuzov Institute of Organic and Physical Chemistry, Russian Academy of Sciences) demonstrated the biological activity of these substances. For the first time, it was shown that nitroxide methanofullerenes in combination with the drug cyclophosphamide exhibit the anticancer activity against leukemia, although the usage of cyclophosphamide alone at the same dose gives no positive effect [14].

In this paper, we study physical–chemical properties of exohedral fullerenes with one and two stable nitroxide biradicals in their composition which can illuminate the processes which take place in such systems. Our interest in nitroxide derivatives of fullerene induced their potentials as drugs in pharmacology and functional materials in optoelectronics. It is known that fullerene after photoexcitation turns into the paramagnetic excited triplet state with electron spin 1. The strong exchange interaction with polynitroxide of fullerene derivatives leads to a more complex multiplet structure of the total system [17, 18].

On the initial step of our work we studied fullerene C_{60} adducts with 2 and 4 covalently linked nitroxide radicals in liquid phase. Since the photophysical and physicochemical properties of fullerenes depend on the attached groups and their interaction, we studied the C_{60} fullerene derivatives with one or two covalently bound nitroxide biradicals at different positions in the solution by continuous-wave EPR spectroscopy.

2 Experimental

2.1 Synthesis of Fullerene Derivatives

Taking into account the results obtained earlier [14, 19], two new bis-methanofullerenes with the addition of the second addend at positions e (equatorial) and trans-3 (Fig. 1) were synthesized and characterized using the Bingel sequential cyclopropanation reaction.

The high-performance liquid chromatography (HPLC) study was performed on an Agilent Technologies 1200 Series chromatograph with a UV detector using a C_{18} reverse phase column (Partisil-5 ODS-3), eluent toluene/CH_3CN (volume ratio 1:1). Organic solvents were used dried and distilled according to standard procedures

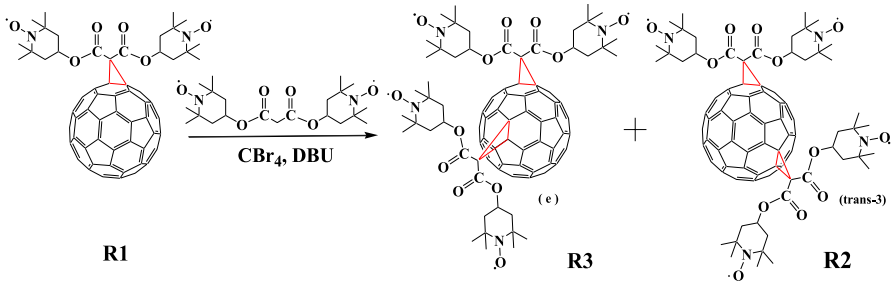

Fig. 1 Scheme of the synthesis of bis-methanofullerenes with the addition of the second addend at positions e (**R3**) and trans-3 (**R2**) to the initial methanofullerene (**R1**)

[20]. We used fullerene C_{60} 99.9% pure (manufactured by Fullerene Center, Nizhny Novgorod, Russia).

To a solution of 0.3 g (0.26 mmol) of methanofullerene (**R1**) in 200 ml of toluene was added 0.164 g (0.39 mmol) of bis (4-carboxy-2,2,6,6-tetramethylpiperidin-1-oxyl)methane in 10 ml of toluene, 0.132 g (0.39 mmol) CBr_4 in 10 ml of toluene, 0.060 g (0.39 mmol) of 1,8-diazabicyclo[5.4.0]undec-7-ene (DBU) in 10 ml of toluene. The reaction mixture was stirred at room temperature for 7 h (during this time, the starting monoadduct almost completely reacted according to HPLC data). The reaction mixture was filtered, washed with distilled water (2×25 ml) and concentrated to minimum. The reaction products were isolated by column chromatography on silica gel with toluene-hexane-acetonitrile as eluent in different ratios. According to the HPLC results, the relative yield of each isomer was: trans-3—16.8%, e—27.6%; real yields for each regioisomer: trans-3—11.2% (45.6 mg), e—18.0% (73.4 mg).

It should be noted that methanofullerene **R1** is a biradical system and bis-methanofullerenes **R2** and **R3** are a tetraradical one.

2.2 EPR Measurements

In this paper, we first studied tetranitroxide derivatives of fullerene C_{60} (**R2** and **R3**) by EPR spectroscopy. Obtained EPR data were compared with the known methanofullerene **R1.**

All experiments were performed at X-band frequencies on an EMX plus spectrometer (Bruker) equipped with a cylindrical super high sensitivity ER 4122SHQE probehead. An ER4131VT temperature unit was used to perform temperature measurements in the temperature range of 250–350 K. All simulations were performed using Matlab and Mathematica program products.

Toluene was selected for liquid-phase measurements as a low-viscous and nonpolar solvent, in which all samples are well dissolved. It was carefully purified according to the literature procedure. Radical concentrations were sufficiently low ($\leq 5\times10^{-4}$ mol l^{-1}) to eliminate intermolecular exchange broadening of EPR lines [21]. Samples were degassed by several freeze/thaw cycles to remove oxygen.

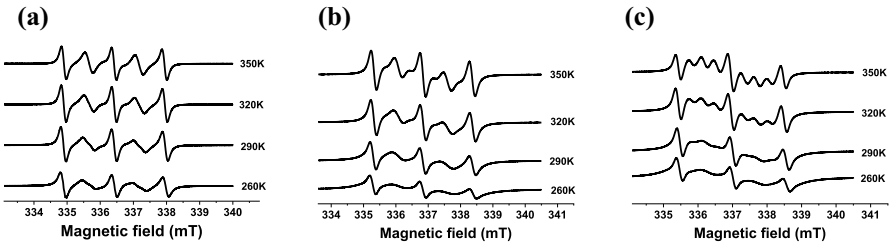

Fig. 2 Temperature dependence of EPR spectra for **R1** (**a**), **R2** (**b**), and **R3** (**c**)

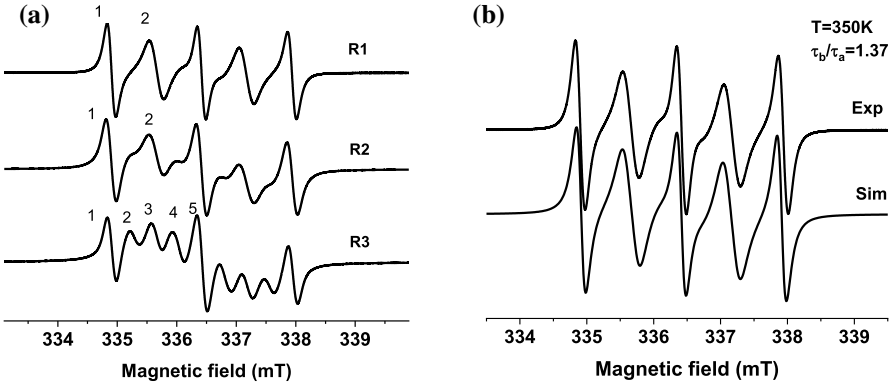

Fig. 3 **a** EPR spectra of **R1**, **R2**, and **R3** in toluene solution at 350 K. To calculate the thermodynamic parameters, the EPR spectrum lines are numbered from left to right. **b** Experimental (Exp) and simulated (Sim) EPR spectra of biradical **R1**. Simulation parameters: $g=2.006$, $a_N=42$ MHz, $\tau_b=1.37$ τ_a, $J_a=0$, $J_b=6a_N$, $p_{ab}=p_{ba}=0.5$. Moreover, EPR spectra of biradical **R1** and tetraradical **R2** are almost the same (see Figs. 2 and 3a)

3 Results and Discussion

3.1 EPR Spectra

Figure 2 shows the temperature dependence of the EPR spectra for **R1**, **R2**, and **R3**. The EPR spectra of the systems **R1** and **R2** consist of resolved five lines in the total temperature range of 260–350 K, while the EPR spectra of the system **R3** have five lines at lower temperatures (260–290 K) and nine lines at higher temperatures (300–350 K).

Figure 3a shows the EPR spectra of all samples at 350 K.

To explain experimental results, we consider polyradical systems in liquids. It is well known that an EPR spectrum of a nitroxide radical like TEMPOL in liquid solution and at low concentration consists of three well-resolved lines due to the hyperfine interaction (HFI) with nitrogen nuclei ^{14}**N** ($I=1$) with the intensity ratio

of 1:1:1 (the super HFI interaction due to protons is disregarded) and the total spectrum width of $2a_N$. The EPR spectrum of a polyradical, in particular a biradical, depends on the spin–spin interaction between the radicals. In [22], it was found that the EPR spectrum depends on the relation between the exchange interaction J and the HFI constant a_N. When $J \sim 0$, the EPR spectrum of a biradical coincides with that of a radical. When the J value increases, additional lines appear and the total spectrum width increases (see Fig. S1a and S2 in Supplementary Material). We note that the lines appearing to the right and to the left of the extreme components of the EPR spectrum of the radical due to the so-called "forbidden transitions" move away from them with increasing J, while their intensity decreases. The maximum possible number of 15 lines is observed in the range of $J/a_N \sim 1$–2 [22–24]. In the case $J >> a_N$, the EPR spectrum of the biradical consists of five lines with the intensity ratio of 1:2:3:2:1 and the total EPR spectrum width is $2a_N$ [22–24].

The same situation is implemented for the tetraradical. In the case of $J \sim 0$, the EPR spectrum of the tetraradical is the same as that for the radical. In the case of $J_{12} \sim J_{13} \sim J_{14} \sim J_{23} \sim J_{24} \sim J_{34} >> a_N$, the EPR spectrum consists of nine lines with the intensity ratio of 1:4:10:16:19:16:10:4:1 [24], where J_{ij} is the exchange interaction between the paramagnetic centers i and j (see Fig. S1b in Supplementary Material).

Figure 2a shows the EPR spectrum of biradical **R1** consisting of five lines, however, its intensity ratio does not correspond to the case $J >> a_N$. This also does not correspond to the situation with $0 < J < a$, because the EPR spectrum does not contain more lines than that for the limiting case $J >> a_N$, namely, five lines for the biradical and nine lines for the tetraradical. Moreover, the total spectrum width corresponds to the spectrum width of a nitroxide radical. This situation is very similar to a model with conformational changes [24–26]. In this model, it is assumed that the studied systems have several metastable conformations. In the simple case, we assume that **R1** has two conformations a and b with $J_a \sim 0$ and $J_b >> a_N$. The lifetimes of these conformations are determined by τ_a and τ_b, respectively. In the literature, the a conformation is named as "far" and the b conformation is known as "close" [25].

Using the dynamical model of a biradical, it is easy to calculate the shape of the EPR spectrum [27]. Let each conformation correspond to certain exchange integrals J_a and J_b, $J_{a,b} << kT$, i.e., the exchange interactions do not affect the dynamics of the conformational transitions. Then, the dynamic equations for the joint spin density matrices ρ_a and ρ_b, which described the conformations a and b, can be written as follows:

$$\frac{\partial \rho_a}{\partial t} = \frac{i}{h}\left[\rho_a, H_a\right] - k_{ab}\rho_a + k_{ba}\rho_b = 0,$$

$$\frac{\partial \rho_b}{\partial t} = \frac{i}{h}\left[\rho_b, H_b\right] - k_{ba}\rho_b + k_{ab}\rho_a = 0,$$

where $k_{ab} = \frac{p_{ab}}{\tau_a}$, $k_{ba} = \frac{p_{ba}}{\tau_b}$, here k_{ij} and p_{ij} are the transition rate and transition probability from the conformation i to the conformation j, respectively.

In the rotating frame, the Hamiltonian of each conformation is written as follows:

$$H_j = \left(\omega_e{}^{(1)} - \omega\right) S_Z{}^{(1)} + \left(\omega_e{}^{(2)} - \omega\right) S_Z{}^{(2)} + a_j{}^{(1)} I_Z{}^{(1)} S_Z{}^{(1)} + a_j{}^{(2)} I_Z{}^{(2)} S_Z{}^{(2)} + \boldsymbol{J_j S}^{(1)} \boldsymbol{S}^{(2)} + \omega_S{}^{(1)} S_X{}^{(1)} + \omega_S{}^{(2)} S_X{}^{(2)},$$

where $\omega_e{}^{(1)}$ is the electron resonance frequency; $a_j{}^{(k)}$ is the HFI constant in the conformation j; $\omega_s{}^{(k)}$ is the microwave frequency ($k = 1, 2$; $j = a, b$), and J_j is the exchange coupling in the conformation j.

The EPR signal in this situation is determined by

$$EPR_{signal} = Sp\left[\left(\rho_a + \rho_b\right)\left(S_X{}^{(1)} + S_X{}^{(2)}\right)\right].$$

Figure 3b shows the experimental and simulated spectra of **R1** at 350 K. The model of conformational changes is in good agreement with the experiment when the ratio $\tau_b/\tau_a = 1.37$ is used.

In this model, it is possible to simulate the EPR spectrum of the tetraradical compound **R2**. This fact indicates that biradicals in **R2** do not interact with each other. The EPR spectrum of **R3** consists of nine lines and this indicates that biradicals interact with each other. However, the intensity ratio is far from being 1:4:10:16:19:16:10:4:1. This distinction makes it possible to consider several conformations and their transition into each other. Unfortunately, the model of two conformations like that used above gives no appropriate simulation of the experimental data.

In the literature, there are many works which made it possible to obtain thermodynamic parameters of transitions of the studied compounds from one conformation to another using the temperature dependence of EPR spectra [24]. This approach was proposed for biradicals in [28], which are extended to triradical and tetraradical systems [24].

In this study, we used the EPR lines marked in Fig. 3a as a basis to determine the thermodynamic parameters. For example, line pairs 1–5 and 2–4 (the central line is not taken into account) are considered for the biradical **R1**.

For biradical **R1** and tetraradical **R2**, the intensity of the lines 1 and 2 reflects ratio of the lifetime in the conformation with $J \sim 0$ to the total measurement time, thus:

$$I_1^a = \frac{\tau_a}{\tau_a + \tau_b} \frac{I}{3}, I_2^a = 0,$$

where $\tau_{a(b)}$ is the lifetime of the molecule in the conformation a (b), I is the total integral intensity of the EPR spectrum. The factor 1/3 reflects the fact that the

intensity of the first line with respect to the total intensity of the EPR spectrum is three times smaller in the case of the conformation *a*.

It is possible to obtain the same expressions in the conformation *b*:

$$I_1^b = \frac{\tau_b}{\tau_a + \tau_b}\frac{I}{9}, I_2^b = \frac{\tau_b}{\tau_a + \tau_b}\frac{2I}{9}.$$

The coefficients of 1/9 and 2/9 in this case appear due to the fact that in the case $J >> a_N$, the first and second lines have a five-component EPR spectrum with the intensities 1 and 2, respectively.

The total intensity of two lines is given by

$$I_1 = I_1^a + I_1^b = \frac{3\tau_a + \tau_b}{\tau_a + \tau_b}\frac{I}{9}, I_2 = I_2^a + I_2^b = \frac{\tau_b}{\tau_a + \tau_b}\frac{2I}{9}$$

and finally, we get

$$\frac{I_2}{I_1} = \frac{2\tau_b}{3\tau_a + \tau_b}, \frac{\tau_b}{\tau_a} = \frac{3(I_2/I_1)}{2 - (I_2/I_1)},$$

where I_1 is the average integral intensity of the lines 1 and 5, I_2 is the average integral intensity of the lines 2 and 4 defined as described in [24, 25].

The ratios $\frac{I_2}{I_1}$ were found for all of the EPR spectra at different temperatures. We note that Fig. 2 shows the EPR spectra only at four temperatures for less cluttering of the figure. The Arrhenius dependence $\ln(\tau_b/\tau_a)$ as function of $1/T$ was plotted after the treatment of the temperature dependence of the EPR spectra. It is known that entropy and enthalpy determine the Gibbs energy $\Delta G = \Delta H - T\Delta S$, where ΔH is enthalpy, ΔS is entropy, T is temperature. On the other hand, $\Delta G = -RTlnK$, where R is the gas constant, T is temperature, K is a factor of equilibrium. In this case, $K = \tau_b/\tau_a$. Solving the last equation for lnK, we get

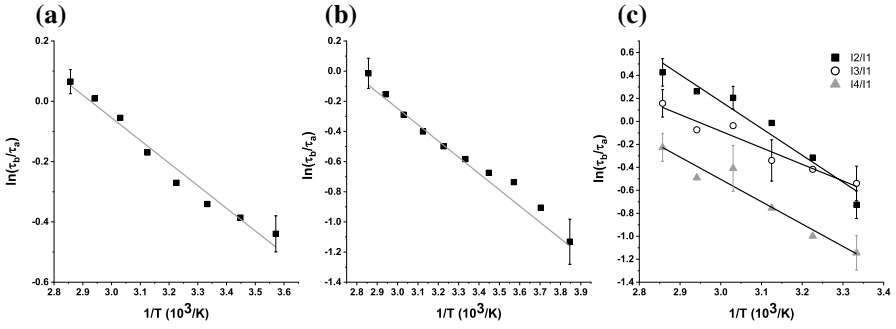

Fig. 4 Arrhenius plots of biradical **R1** (**a**), tetraradicals **R2** (**b**) and **R3** (**c**). Arrhenius plot of **R3** (**c**), obtained for three ratios I_2/I_1 (black square), I_3/I_1 (open cycles), I_4/I_1 (gray triangles)

$$\ln\left(\frac{\tau_b}{\tau_a}\right) = -\frac{\Delta H}{RT} + \frac{\Delta S}{R}.$$

Neglecting the temperature dependence of enthalpy and entropy, we find that in the coordinate system $ln\left(\frac{\tau_b}{\tau_a}\right)$ vs. $1/T$, the temperature dependence of the equilibrium constant is shown by a straight line whose parameters are the slope of $-\Delta H/R$ and intercept of $\Delta S/R$.

Figure 4 shows the Arrhenius plots of biradical **R1** (Fig. 4a) and tetraradical **R2** (Fig. 4b).

Figure 4 shows that the ratio τ_b/τ_a increases with increasing temperature, and consequently, the residence time of the molecule in the conformation b is increased. This result is in good agreement with the temperature dependence of the EPR spectra: the temperature increase leads to the increase in the intensity of line 2 with respect to line 1 (see Fig. 2a and b).

The experimental points were approximated by a linear dependence to determine the thermodynamic parameters. The result is presented in Table 1. Table 1 shows that the entropy (enthalpy) values of **R1** and **R2** do not differ significantly from each other. This fact indicates that the assumption of conformational changes between two conformations and the absence of interaction between the biradicals in **R2** is true.

For the nitroxide tetraradical **R3,** the same step was applied. In our consideration, only two conformational models are taken into account. We used the same expression as given in [25]:

$$\frac{\tau_b}{\tau_a} = \frac{27(I_2/I_1)}{4-(I_2/I_1)}\frac{\tau_b}{\tau_a} = \frac{27(I_3/I_1)}{10-(I_3/I_1)}\frac{\tau_b}{\tau_a} = \frac{27(I_4/I_1)}{16-(I_4/I_1)}.$$

Figure 4c shows the Arrhenius plot for the tetraradical **R3** using different ratios I_3/I_1, I_2/I_1, I_4/I_1.

Figure 4c indicates that for **R3**, the residence time of the molecule in the conformation with larger exchange interaction values increases with the increase in temperature.

Table 1 shows the entropy and enthalpy values of three nitroxide polyradicals. Three sets of the thermodynamic parameters are obtained for the tetraradical **R3**. Moreover, the difference of entropy and enthalpy values is great

Table 1 Thermodynamic parameters of **R1**, **R2** and **R3**

System	I_2/I_1		I_3/I_1		I_4/I_1	
	$\Delta H \pm 0.4$, kJ/mol	$\Delta S \pm 5$, J/(K*mol)	$\Delta H \pm 0.4$, kJ/mol	$\Delta S \pm 5$, J/(K*mol)	$\Delta H \pm 0.4$, kJ/mol	$\Delta S \pm 5$, J/(K*mol)
R1	8.0	24	–	–	–	–
R2	9.0	25	–	–	–	–
R3	19.8	61	12.2	36	16.3	45

(discrepancy > 20%). This is probably due to the assumption that only two conformation models are implemented in the tetraradical **R3**. Probably this assumption is wrong and it is needed to take into account more conformations.

4 Conclusions

In this work, several radical adducts of fullerene C_{60} were studied. The temperature dependence of the EPR line shape was analyzed for all samples and thermodynamic parameters of the fullerene C_{60} derivatives in the solution were obtained. As a result, it is concluded that nitroxide biradicals in bis-methanofullerene **R2** do not interact with each other. It is found that for **R1** and **R2**, the exchange interaction occurs only between radical fragments inside the biradical. The positive enthalpy ΔH value indicates the endothermic nature of the transition between the "far" and "close" conformations. The "far" conformation is the more stable one.

Since entropy ΔS is a measure of ordering of the system, the positive ΔS value and its increasing for bis-methanofullerene **R3** (equatorial isomer of fullerene C_{60} adduct) shows the increase in the system disorder. Since the thermodynamic parameters for the tetraradical **R3** obtained from the analysis of different components of the EPR spectrum do not coincide with each other, it is possible that the model of the two conformations does not fit. Later, we will try to obtain some expressions and simulations for the tetraradical in the case of conformational changes with the number of conformations larger than two.

Supplementary Information The online version contains supplementary material available at https://doi.org/10.1007/s00723-021-01419-x.

References

1. P. Anilkumar, F. Lu, L. Cao, P.G. Luo, J.-H. Liu, S. Sahu, K.N. Tackett Ii, Y. Wang, Y.-P. Sun, Curr. Med. Chem. **18**, 2045 (2011)
2. E. Castro, A.H. Garcia, G. Zavala, L. Echegoyen, J. Mater. Chem. B **5**, 6523 (2017)
3. M. Sosnowska, M. Kutwin, S. Jaworski, B. Strojny, M. Wierzbicki, J. Szczepaniak, M. Łojkowski, W. Święszkowski, J. Bałaban, A. Chwalibog, E. Sawosz, Int. J. Nanomed. **14**, 6197 (2019)
4. A. Barranger, L.M. Langan, V. Sharma, G.A. Rance, Y. Aminot, N.J. Weston, F. Akcha, M.N. Moore, V.M. Arlt, A.N. Khlobystov, J.W. Readman, A.N. Jha, Nanomaterials **9**, 987 (2019)
5. N. Kashef, Y.Y. Huang, M.R. Hamblin, Nanophotonics **6**, 853 (2017)
6. S.K. Sharma, L.Y. Chiang, M.R. Hamblin, Nanomedicine **6**, 1813 (2011)
7. D.Y. Yang, M.F. Wang, I.L. Chen, Y.C. Chan, M.S. Lee, F.C. Cheng, Neurosci. Lett. **311**, 121 (2001)
8. A.Y. Belik, A.Y. Rybkin, N.S. Goryachev, A.P. Sadkov, N.V. Filatova, A.G. Buyanovskaya, V.N. Talanova, Z.S. Klemenkova, V.S. Romanova, M.O. Koifman, A.A. Terentiev, A.I. Kotelnikov, Spectrochim. Acta Part A Mol. Biomol. Spectrosc. **260**, 119885 (2021)
9. A. Hirsch, *The Chemistry of the Fullerenes* (Thieme, New York, 1994)
10. S.H. Friedman, D.L. DeCamp, R.P. Sijbesma, G. Srdanov, F. Wudl, G.L. Kenyon, J. Am. Chem. Soc. **115**, 6506 (1993)
11. O.A. Kraevaya, A.S. Peregudov, I.A. Godovikov, E.V. Shchurik, V.M. Martynenko, A.F. Shestakov, J. Balzarini, D. Schols, P.A. Troshin, Chem. Commun. **56**, 1179 (2020)

12. E. Castro, Z.S. Martinez, C.S. Seong, A. Cabrera-Espinoza, M. Ruiz, A. Hernandez Garcia, F. Valdez, M. Llano, L. Echegoyen, J. Med. Chem. **59**, 10963 (2016)
13. H.A. Beejapur, V. Campisciano, P. Franchi, M. Lucarini, F. Giacalone, M. Gruttadauria, ChemCatChem **6**, 2419 (2014)
14. V.P. Gubskaya, L.S. Berezhnaya, A.T. Gubaidullin, I.I. Faingold, R.A. Kotelnikova, N.P. Konovalova, V.I. Morozov, I.A. Litvinov, I.A. Nuretdinov, Org. Biomol. Chem. **5**, 976 (2007)
15. Y. Li, T. Wang, C. Zhao, Y. Qin, H. Meng, M. Nie, L. Jiang, C. Wang, Dalton Trans. **46**, 8938 (2017)
16. G. I. Likhtenschtein, *Nitroxides. Brief History, Fundamentals, and Recent Developments*, (Springer, Switzerland, 2020)
17. N. Mizuochi, Y. Ohba, S. Yamauchi, J. Chem. Phys. **111**, 3479 (1999)
18. L. Franco, M. Mazzoni, C. Corvaja, V.P. Gubskaya, L.S. Berezhnaya, I.A. Nuretdinov, Appl. Magn. Reson. **30**, 577 (2006)
19. L. S. Berezhnaya, Ph.D. Thesis, Arbuzov Institute of Organic and Physical Chemistry, Russian academy of Sciences, Kazan, Russia, 2009
20. A.J. Gordon, R.A. Ford, *The Chemist's Companion: A Handbook of Practical Data, Techniques, and References* (Wiley, New York, 1973)
21. Y.N. Molin, K.M. Salikhov, K.I. Zamaraev, *Spin Exchange in Chemistry and Biology* (Springer, Berlin, 1980)
22. V.N. Parmon, A.I. Kokorin, G.M. Zhidomirov, J. Struct. Chem. **18**, 104 (1977)
23. R.B. Zaripov, I.T. Khairutdinov, T. Kálai, K. Kish, A.I. Kokorin, K.M. Salikhov, Appl. Magn. Reson. **51**, 523 (2020)
24. M.F. Ottaviani, A. Modelli, O. Zeika, S. Jockusch, A. Moscatelli, N.J. Turro, J. Phys. Chem. A **116**, 174 (2012)
25. V.A. Tran, K. Rasmussen, G. Grampp, A.I. Kokorin, Appl. Magn. Reson. **32**, 395 (2007)
26. K. Komaguchi, T. Iida, Y. Goh, J. Ohshita, A. Kunai, M. Shiotani, Chem. Phys. Lett. **387**, 327 (2004)
27. V.N. Parmon, G.M. Zhidomirov, Mol. Phys. **27**, 367 (1974)
28. V.A. Tran, A.I. Kokorin, G. Grampp, K. Rasmussen, Appl. Magn. Reson. **35**, 389 (2009)